ALGORITHMIC OPTIONS FOR JOINT TIME – FREQUENCY ANALYSIS IN STRUCTURAL DYNAMICS APPLICATIONS

Pol D. Spanos[1], Agathoklis Giaralis[2] and Nikolaos P. Politis[3]

[1]L. B. Ryon Chair in Engineering
Rice University
MS 321, P.O. BOX 1892, Houston, TX 77251, U.S.A.
e-mail: spanos@rice.edu

[2]Department of Civil and Environmental Engineering
Rice University
Houston, TX, U.S.A.
e-mail: agavader@rice.edu

[3]BP America Inc.
Houston, TX, U.S.A.
e-mail: nikolaos.politis@bp.com

Keywords: harmonic wavelets, chirplets, intrinsic modes, inelastic response, non-stationary, accelerograms

Abstract. *The purpose of this paper is to present recent research efforts by the authors supporting the superiority of joint time-frequency analysis over the traditional Fourier transform in the study of non-stationary signals commonly encountered in the fields of earthquake engineering, and structural dynamics. In this respect, three distinct signal processing techniques appropriate for the representation of signals in the time-frequency plane are considered. Namely, the harmonic wavelet transform, the adaptive chirplet decomposition, and the empirical mode decomposition, are utilized to analyze certain seismic accelerograms, and structural response records. Numerical examples associated with the inelastic dynamic response of a seismically-excited 3-story benchmark steel-frame building are included to show how the mean-instantaneous-frequency, as derived by the aforementioned techniques, can be used as an indicator of global structural damage.*

1 INTRODUCTION

Typical earthquake accelerograms are inherently non-stationary as their intensity and frequency content evolve with time due to the dispersion of the propagating seismic waves. From a structural dynamics viewpoint, capturing the time-varying dominant frequencies present in a strong ground motion record facilitates the assessment of its structural damage potential. Furthermore, the time histories of certain structural response quantities, such as floor displacements and inter-story drifts of a building under seismic excitation, are also amenable to treatment as non-stationary signals. Their evolving frequency content provides valuable information about the possible level of structural damage caused by the ground motion. Such signals call for a joint time-frequency analysis; for it is clear that they cannot be adequately represented by the ordinary Fourier analysis which provides only the average spectral decomposition of a signal.

During the past two decades the wavelet transform has become a potent analysis tool in data processing that can be used, among other applications, to yield a well defined time-frequency representation of a deterministic signal[1]. Consequently, this transform has drawn the attention of many researchers in structural engineering and vibration related fields[2,3]. Alternatively, adaptive signal processing techniques can be adopted for effectively capturing local variations of signals on the time-frequency domain[4,5,6].

In this context, the wavelet transform incorporating appropriately filtered harmonic wavelets[7] (HWT), the adaptive chirplet transform[8] (ACT), and the empirical mode decomposition[9] (EMD) in conjunction with the Hilbert transform, are employed in the present study for an analysis of certain earthquake accelerograms[3,6] and structural response time series. Previously derived theoretical formulae[3,6] pertaining to the concept of the mean-instantaneous-frequency[10,11] (MIF) are considered. Furthermore, numerical evidence, supplementing that already available in the literature[3,6], is provided to reinforce the claim that tracing the MIF of critical structural response records is an effective way for detecting and monitoring damage to constructed facilities subject to seismic excitations. In this respect, the inelastic response of a 3-story benchmark steel-frame building[12,13] exposed to two historic seismic accelerograms scaled by various factors to simulate undamaged and heavily

damaged conditions is considered. Joint time-frequency representations of these accelerograms and of the associated displacement response records of the first floor of this benchmark structure as obtained by utilizing the HWT, the ACT and the EMD, are derived along with the corresponding time-histories of the MIFs.

2 MATHEMATICAL BACKGROUND

Consider a signal *x(t)* in the time domain satisfying the finite energy condition

$$\int_{-\infty}^{\infty} \left|x(t)\right|^2 dt < \infty . \tag{1}$$

Traditional Fourier analysis decomposes the signal *x(t)* by projecting it onto the basis of trigonometric (sinusoid) functions with varying frequencies ω by means of the Fourier Transform (FT), defined by the equation

$$X(\omega) = \int_{-\infty}^{\infty} x(t) e^{-i\omega t} dt . \tag{2}$$

Note that sinusoids are mapped as delta functions in the frequency domain, achieving the optimum spectral resolution. However, they possess no localization capabilities in the time domain, being non-decaying functions of infinite support. Therefore, the energy density spectrum $|X(\omega)|^2$ depicts the overall frequency content of a signal, but provides no information about the time that each frequency component was present in the signal.

Obviously, alternative analyzing functions featuring finite effective support in both the time and the frequency domain must be employed to obtain a valid distribution of the signal energy on the time- frequency plane. The remainder of this section refers briefly to the most pertinent of the mathematical details of the three signal processing techniques used in the ensuing numerical analyses. In each case, analytical formulae for the computation of the corresponding joint time-frequency representation and mean instantaneous frequency (MIF) of the signal *x(t)* are included.

2.1 Wavelet spectrogram and mean instantaneous frequency via the harmonic wavelet transform

The continuous wavelet transform uses a basis of analyzing functions generated by appropriately scaling and translating in time a single mother wavelet function. Generally, these are oscillatory functions of zero mean and absolutely integrable and square integrable[1].

Newland[14] introduced the special class of harmonic wavelets which are specifically defined to have a box-shaped band limited spectrum. Two indices (m, n), are used to define their finite support in the frequency domain and thus to control their frequency content. Later, the filtered harmonic wavelet scheme was presented by the same author[7] incorporating a Hanning window function in the frequency domain to improve the time localization capabilities of the harmonic wavelet transform in the wavelet mean square map for a given frequency resolution[7,15]. In this case, the wavelet function of scale (m, n) and position (k) in the frequency domain takes the form

$$\Psi_{(m,n),k}(\omega) = \begin{cases} \dfrac{1}{(n-m)}\left(1-\cos\left(\dfrac{\omega - m2\pi}{n-m}\right)\right), & m2\pi \le \omega \le n2\pi \\ 0, \quad \text{elsewhere} \end{cases}, \tag{3}$$

where m and n are assumed to be positive, not necessarily integer numbers. By application of the inverse Fourier transform in Eq. (3) one obtains its complex- valued time domain counterpart[15] with magnitude

$$\left|\psi_{(m,n),k}(t)\right| = \frac{\sin\pi\left(t-\dfrac{k}{n-m}\right)(n-m)}{\pi\left(t-\dfrac{k}{n-m}\right)\left(\left(t-\dfrac{k}{n-m}\right)^2(n-m)^2-1\right)}, \tag{4}$$

and phase

$$\varphi_{(m,n),k}(t) = \pi\left(t - \frac{k}{n-m}\right)(m+n). \tag{5}$$

Strictly speaking, the filtered harmonic wavelets have an infinite support in the time domain as Eqs. (4) and (5) show, but the fairly fast decay that they exhibit, leads to the definition of an effective support, so that the function is assumed to have a finite energy whose concentration depends on (n- m), besides k.

The harmonic wavelet transform (HWT) of a signal satisfying Eq. (1) is given by the equation

$$w_{(m,n),k}(t) = (n-m)\int_{-\infty}^{+\infty} x(t)\psi^{*}_{(m,n),k}(t)dt\,, \tag{6}$$

where the symbol (*) denotes complex conjugation. Then, in analogy to standard time- frequency analysis procedures[11], the wavelet spectrogram (SP) can be defined as

$$SP(t,\omega) = \left|w_{(m,n),k}\right|^2. \tag{7}$$

The latter form constitutes a three-dimensional graphical direct representation of the energy of the signal *x(t)* versus time and frequency. Treating the SP as a joint time-frequency density function, the MIF can be computed by the expression[3]

$$MIF_{SP}(t) = \frac{\int_{\omega} \omega SP(t,\omega)d\omega}{\int_{\omega} SP(t,\omega)d\omega}, \tag{8}$$

which captures the temporal change of the mean value of the frequencies contained in the signal normalized over the whole spectrum.

2.2 Adaptive spectrogram and mean instantaneous frequency via the chirplet decomposition

Reported by Mallat and Zhang[18], and Qian and Chen[8], the matching pursue (MP) algorithm, allows an alternative decomposition of any signal satisfying Eq. 1 involving a linear combination of a set of analyzing functions (dictionary)[19]. Of particular interest is the case of a Gaussian chirplets dictionary for which the MP yields the following adaptive chirplet transform (ACT)

$$x(t) = \sum_{p} A_p h_p(t) \tag{9}$$

of a signal *x(t)*, with the Gaussian chirplet $h_p(t)$ herein a four- parametered function described by the equation

$$h_p(t) = \sqrt[4]{\frac{a_p}{\pi}} e^{\left\{-\frac{a_p}{2}(t-t_p)^2\right\}} e^{i\left\{\frac{\beta_p}{2}(t-t_p)^2\right\}} e^{i\{\omega_p(t-t_p)\}}. \tag{10}$$

This function involves scaling by the parameter α_p, shifting in time and in frequency by t_p and ω_p respectively, and frequency modulating by chirprate β_p[16]. It attains finite support both in the time and in the frequency domain[17], and, thus, it is capable of capturing the local characteristics of highly non-stationary signals in both domains[4,6].

Furthermore, the expansion coefficients Ap are determined by solving the optimization problem

$$\left|A_p\right|^2 = \max_{h_p}\left|\left\langle x_p(t), h_p(t)\right\rangle\right|^2 = \max_{h_p}\left|\int_{-\infty}^{\infty} x_p(t)h_p(t)dt\right|^2, \tag{11}$$

where

$$\begin{cases} x_{p+1}(t) = x_p(t) - A_p h_p(t), & p \neq 0 \\ x_p(t) = x(t), & p = 0 \end{cases}. \tag{12}$$

For the numerical implementation of the MP algorithm, a refinement scheme introduced by Yin et al.[20] is adopted in the present study.

Upon decomposing the signal *x(t)* as above, it can be shown that a valid distribution of the signal energy in the time-frequency domain, namely the adaptive spectrogram (AS), is given by[8]

$$AS(t,\omega)=2\sum_{p}\left|A_p\right|^2 e^{\left\{-a_p\left(t-t_p\right)^2\right\}}e^{\left\{-\frac{1}{a_p}\left[\left(\omega-\omega_p\right)-\beta_p\left(t-t_p\right)\right]^2\right\}}. \tag{13}$$

Furthermore, the MIF can be determined independently of the AS by the expression

$$MIF_{AS}\left(t\right)=\frac{2\sum_{p}\left|A_p\right|^2\sqrt{a_p\pi}\left(\omega_p+\beta_p\left(t-t_p\right)\right)e^{\left\{-a_p\left(t-t_p\right)^2\right\}}}{\sum_{p}\left|A_p\right|^2\sqrt{a_p\pi}e^{\left\{-a_p\left(t-t_p\right)^2\right\}}}. \tag{14}$$

2.3 Hilbert spectrum and mean instantaneous frequency via the empirical mode decomposition

The empirical mode decomposition (EMD) is another numerical algorithmic procedure for joint time-frequency decomposition of non-stationary signals. The signal is decomposed into a finite number of non predefined case-specific functions, the Intrinsic Mode functions (IMFs)[5,21,22]. An IMF is defined[9] as a function which satisfies the following two conditions: (a) the number of its zero crossings and the number of its extrema must be either equal or differ by one and (b) the mean value of the local minima envelope and the local maxima envelopes of the function must be zero.

Specifically, the EMD yields the decomposition

$$x\left(t\right)=\sum_{j=1}^{N}b_j\left(t\right)+r\left(t\right)\approx\sum_{j=1}^{N}b_j\left(t\right) \tag{15}$$

of a signal *x(t)* obeying Eq. 1, where $b_j(t)$ is the jth IMF and r(t) is a non oscillatory residual function of negligible energy which is typically left when applying the EMD to an arbitrary signal. Associated with each IMF is the analytic signal set in polar form as[11]

$$z_j\left(t\right)=c_j\left(t\right)e^{i\vartheta_j(t)}, \tag{16}$$

where

$$c_j\left(t\right)=\sqrt{b_j^2\left(t\right)+\tilde{b}_j^2\left(t\right)} \tag{17}$$

is the magnitude

$$\vartheta_j\left(t\right)=\arctan\frac{\tilde{b}_j\left(t\right)}{b_j\left(t\right)}, \tag{18}$$

is the phase, and

$$\tilde{b}_j\left(t\right)=\frac{1}{\pi}\int\frac{b_j\left(s\right)}{t-s}ds \tag{19}$$

is the Hilbert transform of the jth IMF.

The salient property of the IMFs is that they are mono-component signals and therefore, the instantaneous frequency of the jth IMF at time t is appropriately defined as the derivative of the phase of its analytic signal[10]

$$\omega_j(t) = \dot{\vartheta}_j(t) = \frac{b_j(t)\dot{\tilde{b}}_j(t) - \dot{b}_j(t)\tilde{b}_j(t)}{b_j^2(t) + \tilde{b}_j^2(t)}. \tag{20}$$

where the dot over a symbol denotes differentiation with respect to time.

The analytic signal of the original signal *x(t)* involves the sum of the analytic signals of the IMF components. That is,

$$\hat{x}(t) = \sum_{j=1}^{N} z_j(t) = \sum_{j=1}^{N} c_j(t) e^{i\int \omega_j(t)dt}. \tag{21}$$

Then the Hilbert spectrum of x defined as

$$H_x(t,\omega) = \sum_{j=1}^{N} c_j\left(t, \omega_j(t)\right) = \sum_{j=1}^{N} c_j(t)\,\delta\left(\omega - \omega_j(t)\right) \tag{22}$$

constitutes a time-frequency representation of the signal x(t) and is a combination of the individual Hilbert spectra of each of the analytic IMFs. To this end, it is natural to define the MIF of the original signal as the weighted average of the instantaneous frequencies of the individual IMFs. That is,

$$MIF_{IMF}(t) = \frac{\sum_{j=1}^{N} c_j^2(t)\,\omega_j(t)}{\sum_{j=1}^{N} c_j^2(t)}. \tag{23}$$

In applying the EMD technique to the signals described in the next section, the same settings for the EMD algorithm and the same filtering schemes for the calculation of the instantaneous frequency of the IMFs were used as in[6].

3 NUMERICAL RESULTS

In recent studies[3,6,15], the usefulness and relative efficiency of the ACT, the HWT and the EMD to provide information about the time-frequency characteristics of recorded strong ground motions and of inelastic response records of seismically excited structural systems has been addressed.

In this section, additional studies are reported in a similar context. Specifically, the El Centro (N-S component recorded at the Imperial Valley Irrigation District substation in El Centro, California, during the Imperial Valley, California earthquake of May 18, 1940), shown in the (b) plot of Fig. 1, and the Hachinohe (N-S component recorded at Hachinohe City during the Takochi-oki earthquake of May 16, 1968), shown in the (b) plot of Fig. 2, earthquake records are considered. Inelastic time-history dynamic analysis was performed for the benchmark 3- story steel frame[12,13] of Fig. 3 using as input the aforementioned ground accelerations scaled by various factors to simulate undamaged and heavily damaged conditions. The standard β-Newmark algorithm with the assumption of constant acceleration at each time step (values β=1/4, γ=1/2), was employed for the numerical integration in time. A trilinear hysteresis model for structural member bending was adopted[12].

For completeness and comparison purposes pertinent joint time-frequency representations of the above seismic accelerograms as obtained by the ACT, the HWT and the EMD techniques are given in Figs. 1,2 and 4. In the (a) plot of each of the Figs. 1 and 2 the percentage of the total energy of the signal captured at different frequencies is provided, obtained by standard Fourier transform analysis. The (c) and (e) plots display the three-dimensional ASs as computed by Eq. 13. and SPs as computed by Eq. 7, correspondingly. In the (d) and (f) parts of the aforementioned figures contour plots of the ASs and of the SPs are presented respectively to provide more efficient and practically useful joint time- frequency signal representations. The MIF is superimposed in these last plots, as obtained by Eq. 14 in the case of the AS (plot (d)), and by Eq. 8 in the case of the SP (plot(f)). In Fig. 4 representative Hilbert spectra (Eq. 22) and estimates of the MIF (Eq. 23) based on the intrinsic mode expansion are juxtaposed for both the El Centro and Hachinohe earthquake records.

The same decomposition algorithms used to process the seismic accelerograms were applied to the lateral displacement response signals of the first floor of the frame under consideration as obtained by the previously defined dynamic analysis. In this context, the primary objective herein is to demonstrate the effectiveness of the MIF as a global damage indicator. In this respect, four extreme cases are shown in Figs. 5 through 11 where the

plots included in Figs. 5, 6, 9 and 10 are of the same kind and order as in Fig. 1. In particular, when the imposed excitations are the El Centro and Hachinohe accelerograms reduced by a factor of 0.5, the frame remains in the elastic region (Figs. 5 and 9). On the other hand, when the original El Centro accelerogram and the Hachinohe accelerogram scaled by 2.25 are used as input the frame suffers structural damage manifested by permanent deformation and a large offset component in the Fourier spectrum (Figs. 6 and 10). For reference purposes the first two natural frequencies of the elastic frame are shown on all plots.

As expected, for all the analyses of the elastic cases the MIF oscillates about, roughly, the same mean value which practically coincides with the fundamental natural frequency of the structure. In the cases that the frame undergoes plastic deformations the attained mean value of the MIF is close to the first natural frequency of the frame, only for about the first 10 seconds duration of the excitation. It is clear that during this time segment the MIF averages the product of the effective frequency response function of the structure with the spectrum of the excitation. However, after the 35th second which approximately marks the effective duration of the input seismic signals (practically the rest of the output signals correspond to free vibration responses), the MIF significantly decreases. This indicates an overall decrease of the effective natural frequencies caused by the structural stiffness degradation.

As far as the assessment of the potential of the three methods for providing valid joint time-frequency representations of non linear structural responses is concerned, similar comments as detailed in Spanos et al.[3,6], where the inelastic response of a benchmark 20-story steel frame building was considered, hold; in general all three methods studied constitute viable alternatives for this purpose.

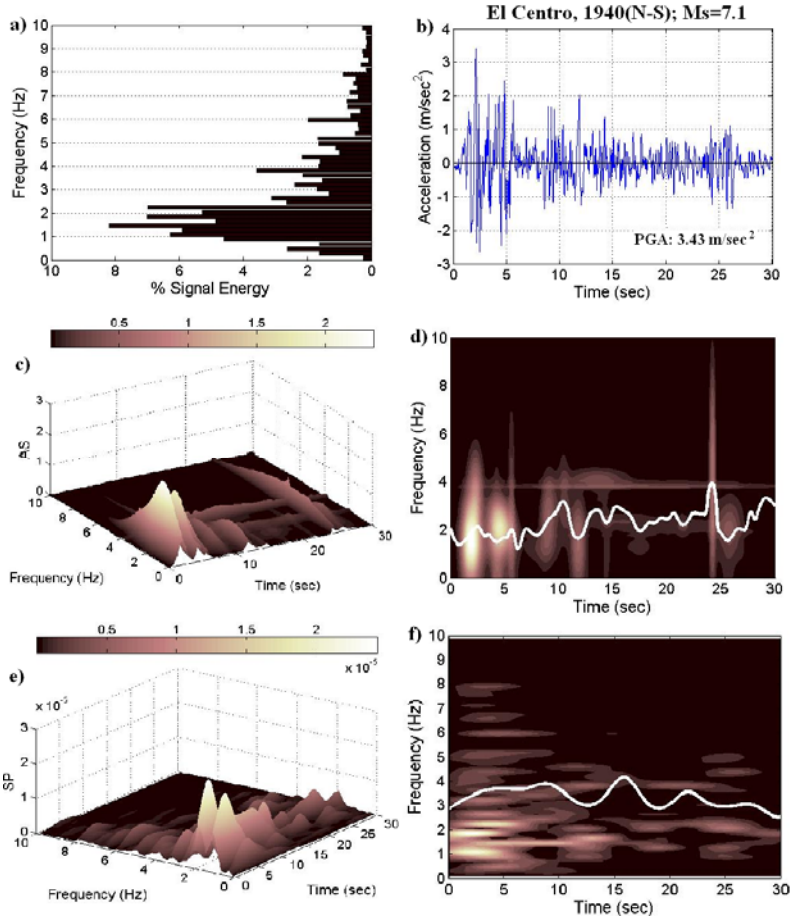

Figure 1. Adaptive chirplet spectrogram (AS) and harmonic wavelet spectrogram (SP) of the El Centro earthquake record; a) Fourier analysis, b) Time-history, c) AS, d) Contour of AS and associated MIF, e) SP, f) Contour of SP and associated MIF.

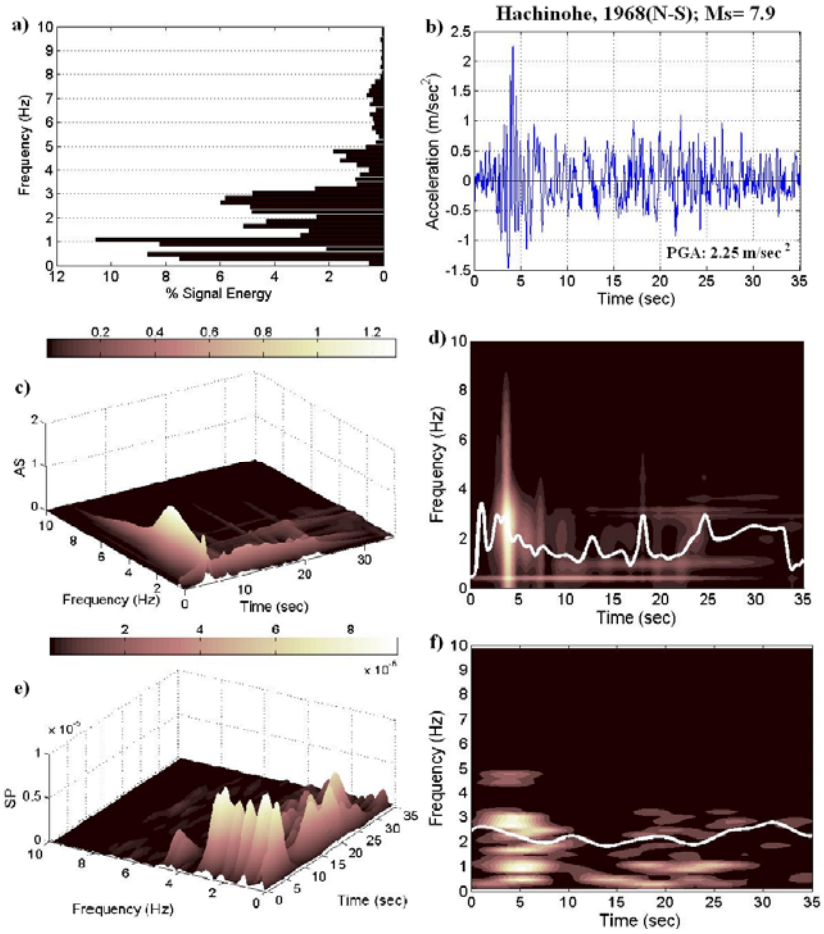

Figure 2. Adaptive chirplet spectrogram (AS) and harmonic wavelet spectrogram (SP) of the Hachinohe earthquake record; a) Fourier analysis, b) Time-history, c) AS, d) Contour of AS and associated MIF, e) SP, f) Contour of SP and associated MIF.

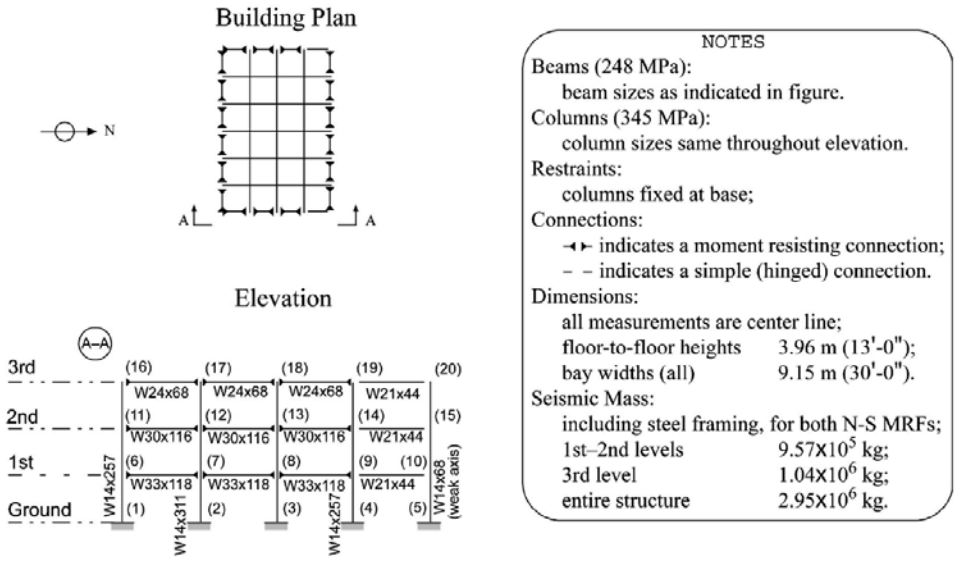

Figure 3. Benchmark 3-story steel frame used in the analysis of typical low-rise building response to earthquake excitations[12].

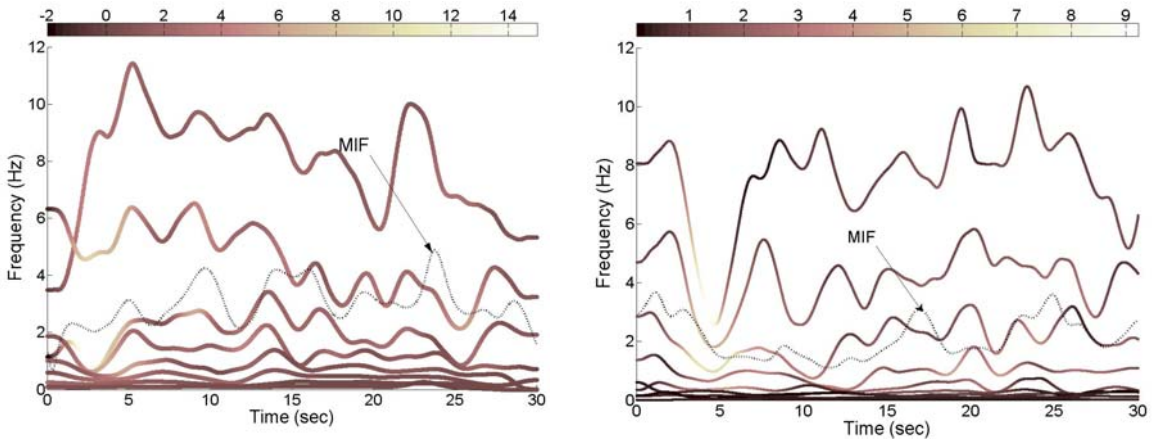

Figure 4. Hilbert spectra via Intrinsic Mode Functions of the El Centro (left plot) and of the Hachinohe (right plot) seismic accelerograms; variation of the instantaneous frequency of the individual IMFs and associated MIF.

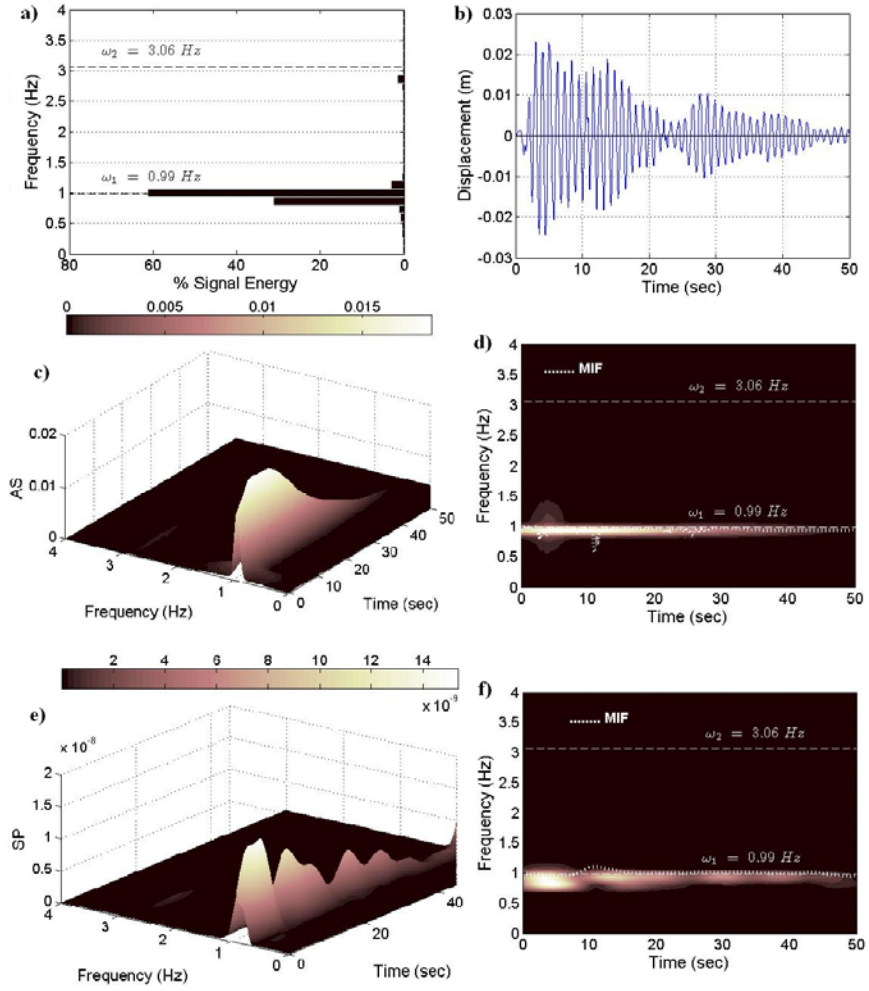

Figure 5. Adaptive chirplet spectrogram (AS) and harmonic wavelet spectrogram (SP) of the first floor lateral displacement response to 0.50· El Centro ground acceleration input; a) Fourier analysis, b) Time-history,

c) AS, d) Contour of AS and associated MIF, e) SP, f) Contour of SP and associated MIF.

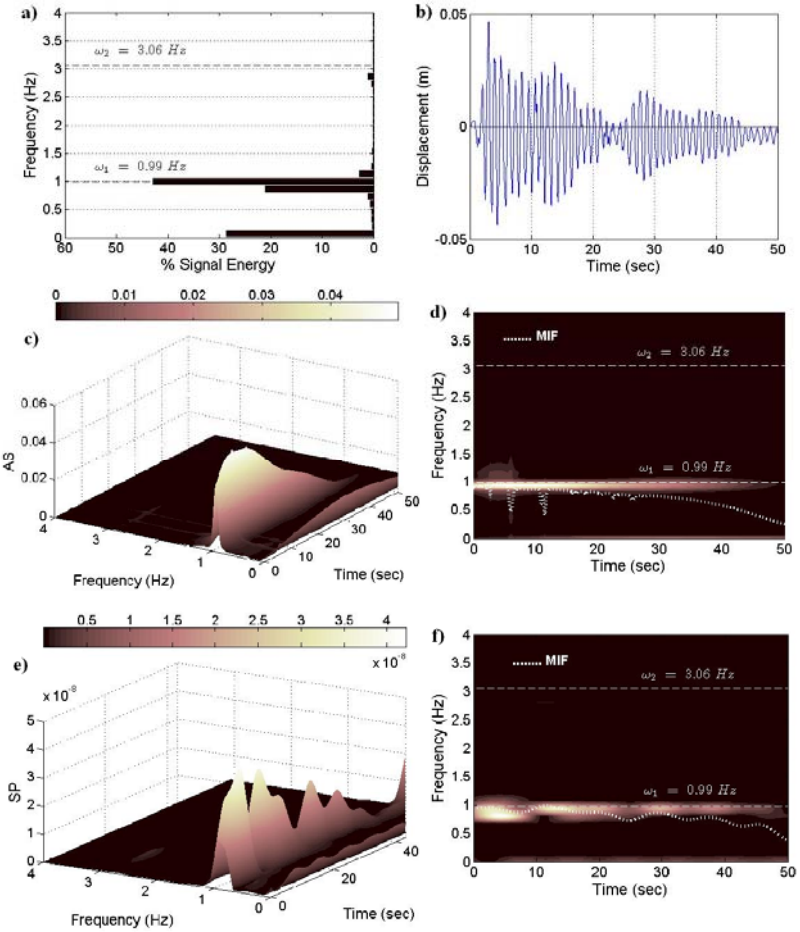

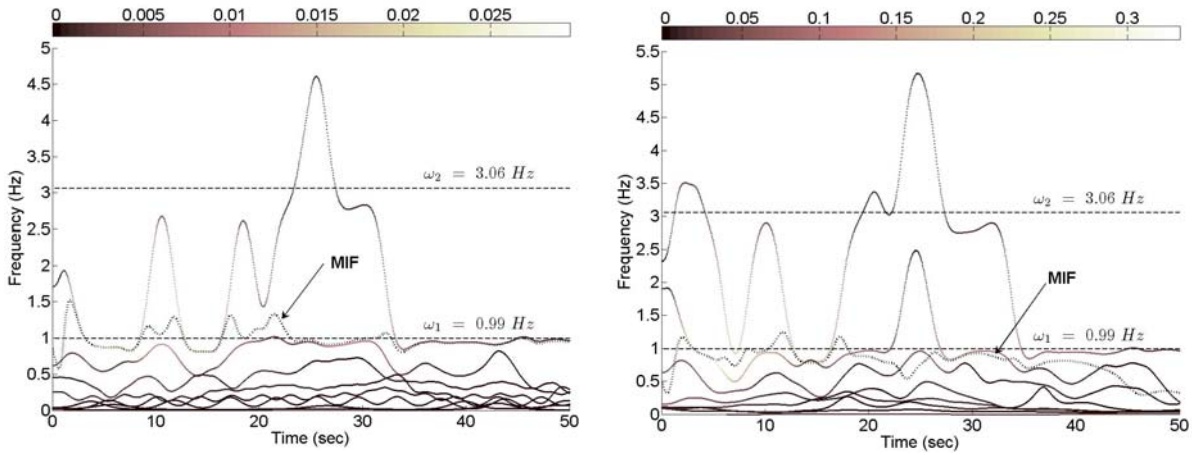

Figure 6. Adaptive chirplet spectrogram (AS) and harmonic wavelet spectrogram (SP) of the first floor lateral displacement response to 1.00· El Centro ground acceleration input; a) Fourier analysis, b) Time-history, c) AS, d) Contour of AS and associated MIF, e) SP, f) Contour of SP and associated MIF.

Figure 8. Hilbert spectra via Intrinsic Mode Functions of the first floor lateral displacement response to 0.50· El Centro (left plot) and 1.00· El Centro (right plot) ground acceleration input; variation of the instantaneous frequency of the individual IMFs and associated MIF.

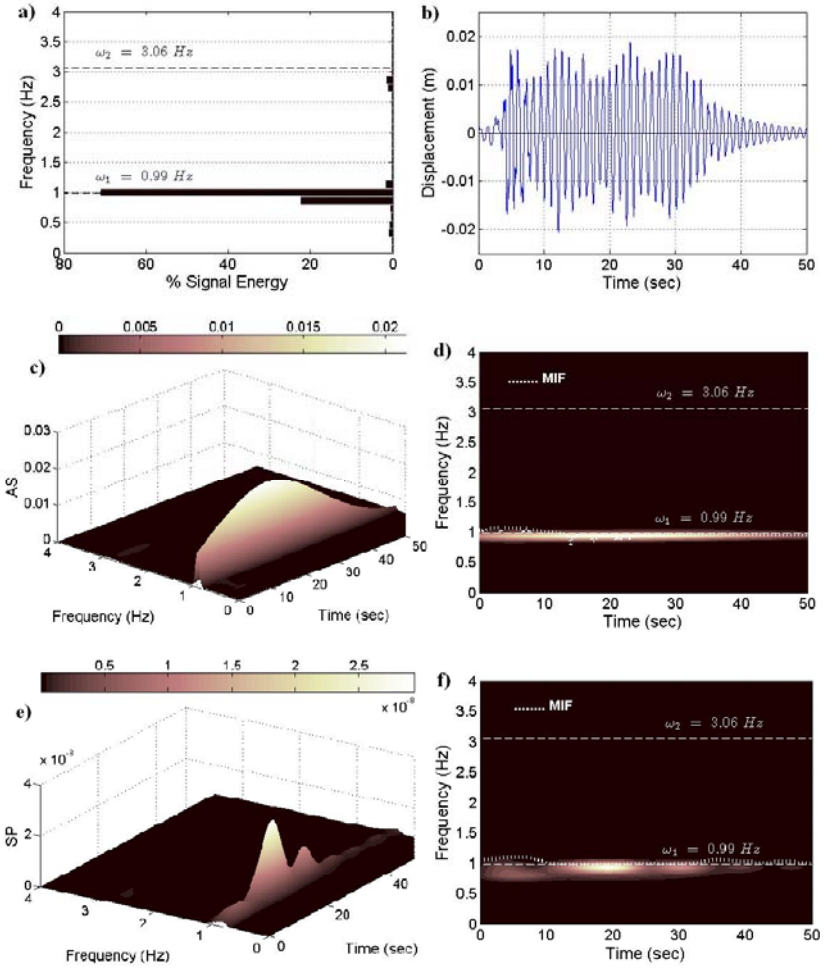

Figure 9. Adaptive chirplet spectrogram (AS) and harmonic wavelet spectrogram (SP) of the first floor lateral displacement response to 0.50· Hachinohe ground acceleration input; a) Fourier analysis, b) Time-history, c) AS, d) Contour of AS and associated MIF, e) SP, f) Contour of SP and associated MIF.

4 CONCLUDING REMARKS

In conjunction with previous research efforts made by the authors[3,6], the present article has addressed the usefulness of using advanced signal processing algorithmic techniques for the joint-time frequency representation of non-stationary signals in earthquake engineering and structural dynamics. Specifically, a non-adaptive (the harmonic wavelet transform), and two adaptive (the chirplet decomposition and the empirical mode decomposition) techniques, have been considered vis-à-vis for analyzing time-histories pertaining to the inelastic response of a benchmark steel-frame structure subject to seismic excitations of various intensities.

Special attention has been given to the concept of the mean instantaneous frequency (MIF) which is inherent to these analyses, and mathematical formulae have been included to facilitate its numerical computation.

It has been found that in the cases where the frame under consideration was forced to exhibit non-linear behavior, the attained values of the MIF were significantly reduced compared to the cases where the frame remained in the elastic region. In this regard, it has been shown that monitoring the mean instantaneous frequency of records of critical structural responses in the context of a time-frequency analysis can be regarded as an effective tool for global structural damage detection, as has been proposed before[3,6]. The latter stems from the ability of the techniques considered herein to capture the influence of nonlinearity on the evolution of the effective natural frequencies of yielding structural systems during a strong ground motion event.

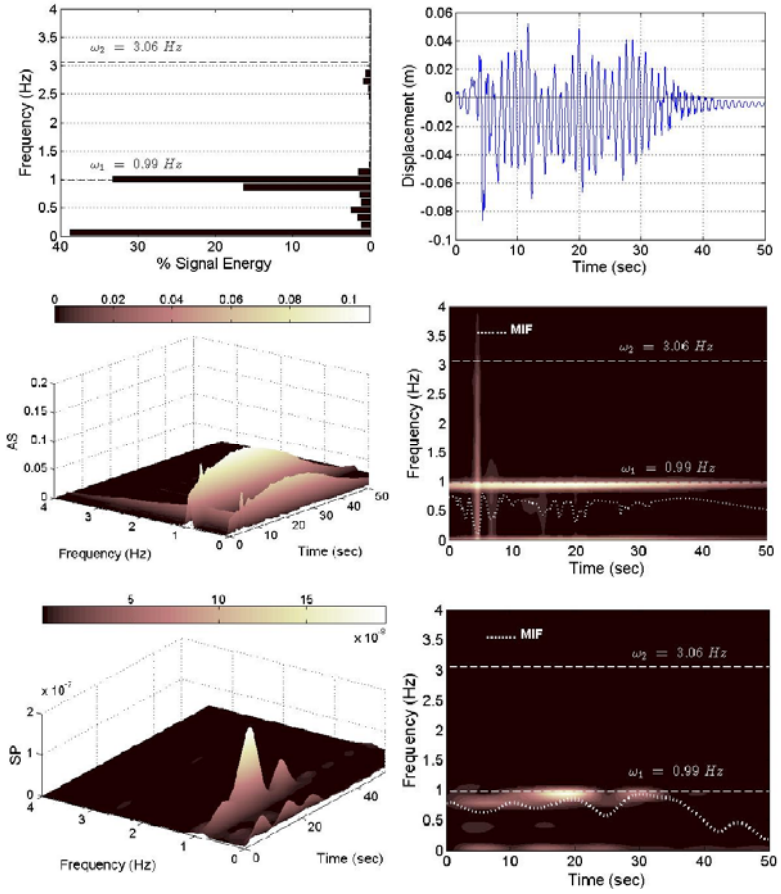

Figure 10. Adaptive chirplet spectrogram (AP) and harmonic wavelet spectrogram (SP) of the first floor lateral displacement response to 2.25· Hachinohe ground acceleration input; a) Fourier analysis, b) Time-history, c) AS, d) Contour of AS and associated MIF, e) SP, f) Contour of SP and associated MIF.

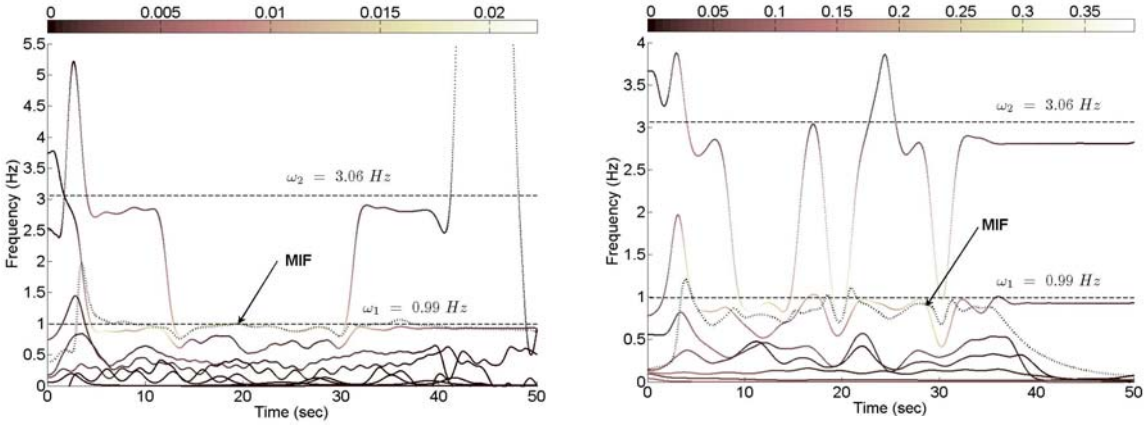

Figure 11. Hilbert spectra via Intrinsic Mode Functions of the first floor lateral displacement response to 0.50· Hachinohe (left plot) and 2.25· Hachinohe (right plot) ground acceleration input; variation of the instantaneous frequency of the individual IMFs and associated MIF.

ACKNOWELEDGEMENTS

The financial support of this work from an NSF grant is gratefully acknowledged.

REFERENCES

[1] Mallat, S. (1998), A Wavelet Tour of Signal Processing, Academic Press, London.
[2] Spanos, P.D. and Failla, G. (2005), "Wavelets: Theoretical concepts and vibrations related applications," Shock Vib. Digest, 37, pp. 359-375.
[3] Spanos, P.D., Giaralis, A., Politis, N.P. and Roessett, J.M. (2007), "Numerical treatment of seismic accelerograms and of inelastic seismic structural responses using harmonic wavelets," Comput. Aided Civil Infrastruct. Eng. 22, pp. 254-264.
[4] Qian, S. (2001), *Introduction to time-frequency and wavelet transforms*, Prentice- Hall, New Jersey.
[5] Huang, N.E. and Attoh-Okine, N.O., eds. (2005), *The Hilbert-Huang transform in engineering,* CRC Press, Boca Raton.
[6] Spanos, P.D., Giaralis, A. and Politis, N.P. (2007), "Time- frequency representation of earthquake accelerograms and inelastic structural response records using the adaptive chirplet decomposition and empirical mode decomposition," Soil Dynam. Earthquake Eng. 27, pp. 675-689.
[7] Newland, D.E. (1999), "Ridge and phase identification in the frequency analysis of transient signals by harmonic wavelets," J. Vib. Acoust. 121, pp. 149-155.
[8] Qian, S. and Chen, D. (1994), "Signal representation via adaptive normalized Gaussian functions," Signal Process 36, pp. 1-11.
[9] Huang, N.E., Shen, Z., Long, S.R., Wu, M.C., Shih, H.H., Zheng, Q., Yen, N.C., Tung, C.C. and Liu, H.H. (1998), "The empirical mode decomposition and the Hilbert spectrum for nonlinear and non-stationary time series analysis," Proc. R. Soc. Lond. A 454, pp. 903-995.
[10] Boashash, B. (1992), "Estimating and interpreting the instantaneous frequency of a signal. I. Fundamentals," Proc. IEEE, 80, pp. 520-538.
[11] Cohen, L. (1995), *Time- Frequency Analysis*, Prentice- Hall, New Jersey.
[12] Ohtori, Y., Christenson, R.E., Spencer, B.F.J. and Dyke, S.J. (2004), "Benchmark structural control problems for seismically excited nonlinear buildings," J. Eng. Mech. 130, pp. 366-385.
[13] Spencer, B.F.J., Christenson, R.E. and Dyke, S.J. (1999), "Next generation benchmark control problems for seismically excited buildings," *Proceedings of the 2nd World Conference on Structural Control*. Vol.2, pp. 1135–1360, Wiley, New York.
[14] Newland, D.E. (1994), "Harmonic and musical wavelets," Proc. R. Soc. Lond. A 444, pp. 605-620.
[15] Spanos, P.D., Tezcan, J. and Tratskas, P. (2005), "Stochastic processes evolutionary spectrum estimation via harmonic wavelets," Comput. Methods Appl. Mech. Eng. 194, pp. 1367-1383.
[16] Mann, S. and Haykin, S. (1995), "The chirplet transform: Physical considerations," IEEE Trans Signal Process. 43, pp. 2745-2761.
[17] Baraniuk, R.G. and Jones, D.L. (1996), "Wigner- based formulation of the chirplet transform," IEEE Trans Signal Process. 44, pp. 3129-3135.
[18] Mallat, S. and Zhang, Z. (1993), "Matching pursuits with time-frequency dictionaries," IEEE Trans Signal Process 41, pp. 3397-3415.
[19] Chen, S.S., Donoho, D.L. and Saunders, M.A. (1998), "Atomic decomposition by basis pursuit," SIAM J. Sci Comput 20, pp. 33-61.
[20] Yin, Q., Qian, S. and Feng, A. (2002), "A fast refinement for adaptive gaussian chirplet decomposition," IEEE Trans Signal Process 50, pp. 1298-1306.
[21] Rilling, G., Flandrin, P. and Goncalves, P. (2003), "On empirical mode decomposition and its algorithms," *IEEE-EURASIP Workshop on nonlinear signal and image processing* NSIP-03, GRADO(I).
[22] Flandrin, P. and Goncalves, P. (2004), "Empirical mode decompositions as data-driven wavelet-like expansions," Int. J. Wavelets Multiresolut. Inform. Process. 2, pp. 477-496.